International Journal of Pharmaceutics 376 (2009) 161–168

Contents lists available at ScienceDirect

International Journal of Pharmaceutics

journal homepage: www.elsevier.com/locate/ijpharm

Pharmaceutical Nanotechnology

Synthesis, characterization, drug-loading capacity and safety of novel octyl modified serum albumin micelles

Jian Gong[1], Meirong Huo[1], Jianping Zhou*, Yong Zhang, Xiaoling Peng, Di Yu, Hui Zhang, Jing Li

Department of Pharmaceutics, China Pharmaceutical University, 24 Tongjiaxiang, Nanjing 210009, China

ARTICLE INFO

Article history:
Received 25 January 2009
Received in revised form 23 March 2009
Accepted 22 April 2009
Available online 3 May 2009

Keywords:
Octyl modified serum albumin (OSA)
Polymeric micelles
Paclitaxel
Drug-loading
Hemolysis
Cytotoxicity

ABSTRACT

A novel albumin derivative octyl modified serum albumin (OSA) which can form a core–shell structure in aqueous media by self-assembling due to core segregation and a combination of intermolecular forces has been synthesized. The chemical structure and physical properties of OSA were characterized by FTIR, ^{1}H NMR and TG. The degree of substitution (DS) was in the range of 52.4–69.7% and 48.9–65.8% determined by elemental analysis and fluorescamine assay, respectively. With the increase in the DS of octyl group, the critical micelle concentration (CMC) decreased from 30.1 to 14.7 mg/L because of the increasing hydrophobicity. In the light of the hydrophobic core as a microreservoir for poorly water-soluble drugs, paclitaxel (PTX) was successfully loaded into OSA micelles by the dialysis method with a high drug-loading (33.1 wt%) and entrapment efficiency (90.5%) due to the synergistic effect of micellar encapsulation and binding interaction between drug and OSA. Compared with PTX-loaded unmodified BSA preparation, PTX-loaded OSA micelles are characterized by small size, narrow size distribution, great drug-loading capacity and enhanced stability. The size of PTX-loaded micelles was in the range of 123.3–152.8 nm and smaller than their corresponding blank micelles. Hemolysis and cytotoxicity studies showed that OSA was safer than Tween-80 and Cremophor EL as an injectable pharmaceutic adjuvant for PTX. In terms of the greater drug-loading capacity and safer character, the novel albumin derivative OSA is a prospective injectable delivery system for PTX.

1. Introduction

Serum albumin is the most abundant protein (5 g/100 mL) in plasma. Its most important physiological role is thought to bring a very wide range of materials to their target organs (Peters, 1985; Carter and Ho, 1994) and maintain pH and colloid osmotic pressure of plasma due to its small size and abundance (Peters, 1985; Figge et al., 1991). It consists of three structurally homologous domains (I, II and III), each of which can be further divided into two subdomains (A and B) (Sugio et al., 1999; Ghuman et al., 2005). The primary regions of various compounds binding sites of albumin are located in subdomains IIA and IIIA, which are characterized by deep hydrophobic pockets with positively charged entrances (He and Carter, 1992; Sugio et al., 1999). In addition to its ordinary clinical applications, many pharmaceutical researchers (Sparreboom et al., 2005; Chemmanur and Wu, 2006; Kratz, 2007) have attempted to utilize albumin as a drug carrier owing to its preferential uptake in tumor and inflamed tissue, ready availability, biodegradability and lack of toxicity and immunogenicity properties. Principally, three drug delivery technologies can be distinguished (Kratz, 2008): coupling of low-molecular weight drugs to exogenous or endogenous albumin, e.g. DOXO-EMCH (Kratz, 2007), conjugation with bioactive proteins to enhance its stability and half-life, such as Albuferon, a fusion protein of albumin and interferon (Chemmanur and Wu, 2006) and encapsulation of drugs into albumin nanoparticles (Sparreboom et al., 2005).

Paclitaxel (PTX) is an effective antineoplastic agent by promoting the assembly of microtubules from tubule dimmers and preventing them from depolarizing (Spencer and Faulds, 1994). Because of its low solubility (0.3 μg/mL), commercially available formulation (Taxol®) is formulated in a 50/50 (v/v) mixture of Cremophor EL (CrmEL)/ethanol. However, CrmEL is biologically and pharmacologically active and the amount of CrmEL required is considerably high, which results in significant side effects (Gelderblom et al., 2001).

Because of the inherent problems associated with CrmEL, some new drug delivery systems (DDSs) for PTX, which have good aqueous solubility and fewer side effects, are under current investigation including emulsion (He et al., 2003), liposomes (Wu et al., 2006), water-soluble prodrugs (Skwarczynski et al., 2006), nanoparticles (Bilensoy et al., 2008), cyclodextrin complexes (Bouquet et al., 2009), polymeric micelles (Zhang et al., 1996; Soga et al., 2005; Kang Moo et al., 2008) and nanoparticle colloidal suspension (Sparreboom et al., 2005). Among these DDSs, the most successful

* Corresponding author. Tel.: +86 25 83271272; fax: +86 25 83301606.
E-mail address: zhoujpcpu@126.com (J. Zhou).
[1] Jian Gong and Meirong Huo contributed equally to this work.

0378-5173/$ – see front matter © 2009 Elsevier B.V. All rights reserved.
doi:10.1016/j.ijpharm.2009.04.033

formulations are Genexol®-PM and Abraxane®. Genexol®-PM is a formulation of PTX in PEO-*b*-PDLLA micelles, which has resulted in a 5000-fold increase in the inherent solubility of PTX in aqueous media (Zhang et al., 1996). Polymeric micelles are formed through the self-assembly of amphiphilic polymers in aqueous media. Due to its small particle size, targeting ability, stability, long circulation and easy production, it received growing scientific attention as a efficient drug carrier in recent years (Kataoka et al., 2001; Aliabadi and Lavasanifar, 2006). Abraxane® is a novel albumin-bound nanoparticle PTX formulation (130 nm) which has been approved by FDA on January 7, 2005 for the chemotherapy of recurrent metastatic breast cancer (Sparreboom et al., 2005). Abraxane® enhances the drug concentration of tumor through EPR effect of tumor (Fang et al., 2003) in combination with receptor-activated transcytosis (Simionescu et al., 2002). The maximum tolerated doses (MTD) of the two formulation are 390 (Kim et al., 2004) and 300 mg/m^2 (Ibrahim et al., 2002), respectively, both of which are higher than that of Taxol®. However, the drug-loadings of reported polymeric micelles (Zhang et al., 1996; Soga et al., 2005) and Abraxane® (Zenoni and Maschio, 2007) were low and the stability of Abraxane® was less than 24 h when the pH was out of the range of 5.4–5.8, an alternative formulation for PTX is needed for medical applications.

Being stimulated by the two formulations and exploring an improved formulation for PTX, we synthesized a series of novel albumin derivative octyl modified serum albumin (OSA) by attaching octyl to the reactable primary amino groups of albumin molecules in order to improve the hydrophobicity of albumin and form a core–shell structure by self-assembling in aqueous media, which consequently leads to a great drug-loading capacity for those poorly water-soluble drugs, such as PTX, camptothecin, itraconazole, indomethacin, nimodipine and so on, because of the encapsulation and binding effect. This study involves synthesis of a series of OSA, chemical structure, physical properties and safety studies, characteristics of OSA micelles and its drug-loading capacity for PTX.

2. Materials and methods

2.1. Materials

Bovine serum albumin (BSA) with a molecular weight of 65,000 and an isoelectric point (p*I*) of 4.7 was purchased from Yumin Biotech Co., Ltd. (Shanghai, China). PTX, fluorescamine and pyrene were purchased from Sunve Pharmaceutical Co., Ltd. (Shanghai, China), Acros (Belgium) and Fluka (USA) company, respectively. Octaldehyde and $NaBH_4$ were obtained from Nanjing Sky Run Perfume Co., Ltd. (Nanjing, China) and Sinopharm Chemical Reagent Co., Ltd. (Shanghai, China) company, respectively. All other chemicals were of analytical grade and were used without further purification.

2.2. Synthesis of OSA

1 g of BSA was dissolved in 50 mL double distilled water with stirring at room temperature, then octaldehyde with varying feed molar ratio to the reactable amino groups (2:1, 4:1, 6:1, 8:1) of BSA was added. 10% $NaBH_4$ solution dissolved in water was added dropwise to the solution 1 h later. The reaction mixture was stirred overnight and neutralized with 2.5 M hydrochloric acid. The solution was dialyzed (MWCO 14000) against phosphate buffer (pH 7.4, 10 mM) for 3 days, followed by ultrafiltration (MWCO 10000) twice with a pressure of 0.18 MPa, then lyophilized and octyl modified serum albumin was obtained (yield ~80%).

2.3. Characterization of OSA

FTIR spectra of BSA and OSA were obtained on FTIR spectrometer (Nicolet 2000) after compressing into KBr pellets, in the range from 4000 to 400 cm^{-1}, with a resolution of 2 cm^{-1}.

^{1}H NMR spectra of BSA and OSA in the solution of D_2O were acquired on a Bruker (AVACE) AV-500 spectrometer.

Degree of substitution (DS) of octyl group of OSA was determined by elemental analysis using an Element Vario EL III analyzer and fluorescamine assay, respectively. However, only the ε-amino group of lysine and the terminal amino group are capable of reacting with aldehyde group, the elemental analysis equation was modified by a correction factor. In this case, we defined 13.36 (815/61) as the correction factor, because there are 815 nitrogen atoms in BSA molecule, while 60 lysines and one terminal amino group (Peters, 1985). So the equation can be described as below:

$$\text{DS of octyl group}\,(\%) = \frac{(C/N)_{\text{OSA}} - (C/N)_{\text{BSA}}}{8} \times 13.36 \times 100$$

Fluorescamine assay was carried out following a procedure reported by (Stocks et al. 1986). Briefly, 5 mg of sample (BSA and OSA) was dissolved in 50 mM phosphate buffer (pH 7.4) as the stock solution. Different volumes (0–0.4 mL) of stock solution were mixed with 0.4 mL of fluorescamine solution (1 mg/mL in acetone) in a series of 10 mL of volumetric flasks, then phosphate buffer (pH 7.4) was added to each volumetric flask to obtain a final volume of 10 mL, finally all solutions were kept for 10 min in the dark. Fluorescence emission intensity was determined on spectrofluorimeter (Shimadzu RF-5301 PC, Japan) at 477 nm with an excitation wavelength of 390 nm. Each curve was generated by plotting sample concentration versus fluorescent intensity. DS of octyl group was determined by the following equation:

$$\text{DS of octyl group}\,(\%) = \left(1 - \frac{\text{slope rate of OSA}}{\text{slope rate of BSA}}\right) \times 100$$

TG analysis was performed with NETZSCH TG 209 equipment. The temperature range was 30–400 °C and the heating rate was 10 °C/min.

2.4. Preparation of OSA micelles and determination of critical micelle concentration (CMC)

OSA micelles were prepared by a direct dissolution and ultrasonication method. Generally, 10 mg of lyophilized OSA powder was dissolved in 5 mL of double distilled water. The solution was ultrasonicated for 10 min (JY 92-IID ultrasonic processor, China) in a cooling bath followed by filtering through a 0.45 μm pore-sized microporous membrane.

Zetasizer 3000 (Malvern, UK) was used to measure the size and zeta potential of polymeric micelles. The morphology of the micelles was further observed by transmission electron microscopy (TEM) by an H-7650 (Hitachi, Japan) transmission electron microscope operating at an accelerating voltage of 80 kV.

CMC of OSA was estimated by the fluorescence spectroscopy, using pyrene as the probe. Briefly, 1 mL of 6.0×10^{-6} M pyrene solution in acetone was added to a series of 10 mL volumetric flask and then acetone was evaporated. 10 mL of different concentrations of OSA solutions (2×10^{-4} to 5 mg/mL) was added to the volumetric flasks followed by sonicating for 30 min. The sample solutions were incubated at 50 °C for 2 h, and then left to cool down overnight at room temperature. Pyrene excitation spectra were recorded on a fluorescent spectrophotometer, with an emission wavelength of 390 nm. Both of the excitation and emission slit-widths were 3 nm.

2.5. Preparation and characterization of PTX-loaded OSA micelles

PTX-loaded micelles were prepared by the dialysis method. 90 mg of OSA was dissolved in 15 mL of water with stirring for 30 min at room temperature. Then 50 mg of PTX dissolved in 1.65 mL of ethanol was added dropwise and sonicated for 30 min (JY 92-IID ultrasonic processor, China) in a cooling bath. The solution was dialyzed against phosphate buffer (pH 7.4) with a dialysis membrane (MWCO 14000) for 10 h followed by centrifuging at 3000 rpm for 10 min, filtering through a 0.45 μm pore-sized microporous membrane and lyophilization. For comparison, PTX-loaded unmodified BSA preparation was also prepared with the same method.

Size, zeta potential and morphology of the PTX-loaded micelles were measured as described in Section 2.4. X-ray diffraction (WAXD) diagrams were performed with an XD-3A powder diffraction meter with Cu Kα radiation in the range of 3–40° (2θ) at 40 kV and 50 mA. Differential scanning calorimeter (DSC) analysis was carried out using NETZSCH DSC 204 equipment with the temperature range and heating rate of 40–300 °C and 10 °C/min, respectively.

The stability of PTX-loaded micelles was also tested in terms of the PTX content and size at 4, 25 and 37 °C. For comparison, the size of blank micelles was also measured in the same condition.

2.6. Determination of drug-loading and entrapment efficiency

The drug-loading and entrapment efficiency were calculated by the following equations:

$$\text{Drug loading}\,(\%) = \frac{\text{weight of PTX in micelles}}{\text{weight of PTX in micelles} + \text{weight of carrier fed initially}} \times 100$$

$$\text{Entrapment efficiency}\,(\%) = \frac{\text{weight of PTX in micelles}}{\text{weight of PTX fed initially}} \times 100$$

The concentration of PTX was determined by isocratic reverse-phase HPLC (Shimadzu LC-2010C system, Kyoto, Japan) equipped with a Lichrospher™ C18 column (5 μm particle size, 250 mm × 4.6 mm). The mobile phase consisted of methanol and water (75:25, v/v) with a flow rate of 1.0 mL/min and the detection wavelength was 227 nm (SPD-10A, UV detector, Shimadzu, Japan). The sample was prepared by dissolving the lyophilized powder in double distilled water and being diluted by the mobile phase (to destroy micelles and dissolve PTX) and 20 μL of the sample was injected. The calibration curve of various PTX concentrations (C, 0.1–20.0 μg/mL) versus integrated area (A, mAU s) was $A = 36852C - 2070.4$, with a correlation coefficient of 0.9999.

2.7. Hemolysis test

Rabbit blood was freshly drawn from arteria cruralis, and the fibrinogen was removed by stirring with a glass rod. Then the blood was washed with 0.9% NaCl, centrifuged at 3000 rpm for 5 min, and followed by removing the supernatant for three times. The red blood cells (RBC) were diluted with 0.9% NaCl to obtain a concentration of 2% (v/v) suspension. The lyophilized power of OSA and PTX-loaded micelles was dissolved in 0.9% NaCl at a concentration of 10 and 0.5 mg/mL, respectively. 2.5 mL of 2% RBC suspension was added to each tube which contained different volumes (0.1–2 mL) of OSA or PTX-loaded micelles solution. Then 0.9% NaCl solution was added in each tube to obtain a final volume of 5 mL. The positive (100% hemolysis) and negative control (0% hemolysis) were obtained by mixing 2.5 mL of water and 0.9% NaCl solution with 2.5 mL of 2% RBC suspension, respectively. The blank groups were prepared without RBC suspension to eliminate the effect of background. For comparison, the vehicle of the commercial PTX formulation CrmEL, the commonly used low-molecular weight surfactant Tween-80 and the commercial PTX formulation were also prepared. Samples were incubated at 37 °C for 30 min, and centrifuged at 3000 rpm for 10 min to remove non-lysed RBC. The supernatant was analyzed by spectrophotometric determination at 540 nm. The degree of hemolysis was determined by the following equation:

$$\text{Hemolysis}\,(\%) = \frac{A_{\text{sample}} - A_{0\%}}{A_{100\%} - A_{0\%}} \times 100$$

2.8. In vitro cytotoxicity studies

100 μL of Hepg2 cell suspension in culture medium (DMEM + 10% FCS) with the concentration of 5×10^4 cells/mL was seeded in each well of 96-well plates, and incubated at 37 °C in a humidified atmosphere with 5% CO_2. PTX-loaded (with PTX concentration of 1 mg/mL) and blank OSA micelles (equivalent concentration of polymer to PTX-loaded micelles) were prepared. For comparison, the commercial PTX formulation Taxol® and the vehicle of Taxol® CrmEL were also prepared. The four stock solutions were further stepwise diluted with PBS (pH 7.4) to give PTX concentrations ranging from 0.0001 to 100 μg/mL. After 24 h of incubation, 100 μL of sample solution was added to each cell. Moreover, 100 μL of PBS (pH 7.4) was added as the reference. The cells were incubated for 72 h at 37 °C in a humidified atmosphere with 5% CO_2. After incubation, 25 μL of a 5 mg/mL MTT solution was added to each well, and the plates were incubated for an additional 4 h. Drop the supernatant and add 100 μL of DMSO to each well to dissolve the formazan crystals. Plates were shaken for 30 min and the optical densities (ODs) were read at 570 nm using a microplate reader (SOFT max® PRO, Molecular Devices Corporation, CA). Cell viability (%) was calculated as (OD of test group/OD of control group) × 100.

3. Results and discussion

3.1. Preparation and characterization of OSA

Serum albumin exhibits favorable biocompatibility and nontoxicity and chemically possesses many active groups, such as primary amino group, carboxyl group and thiol group (Veronese, 2001). In this paper, a series of novel albumin derivative octyl modified serum albumin was synthesized based on the specific reaction between aldehyde group and primary amino group in order to improve the lipophilicity of albumin and form a core–shell structure by self-assembling in aqueous media. By changing the molar ratio of aldehyde group to the reactable amino group of BSA, various OSAs with different DS of octyl group were prepared. The derivative nomenclature is designated OSA-n, where n stands for the molar ratio of aldehyde group to the reactable amino group of BSA.

Fig. 1 shows the FTIR spectra of BSA and OSA-8. Compared with the FTIR spectrum of native BSA (Fig. 1(a)), the peaks of OSA-8 (Fig. 1(b)) increased at 2929.8 cm^{-1} (C–H stretch of methylene) and decreased at 3500–3300 cm^{-1} (N–H stretch of primary amine), which indicates the attachment of octyl group to primary amino group of albumin.

Fig. 2 shows the ^1H NMR spectra of BSA and OSA-8. To OSA-8 (Fig. 2(b)), the peaks at 1.24 and 0.84 ppm were attributive to the methylene and methyl hydrogen, respectively. Because of the complicated structure of albumin and its already existing alkyl group, these differences between BSA and OSA in IR and ^1H NMR spectra were minor.

DS of octyl group of OSA was defined as the number of octyl groups per 100 primary amino groups and was calculated by two

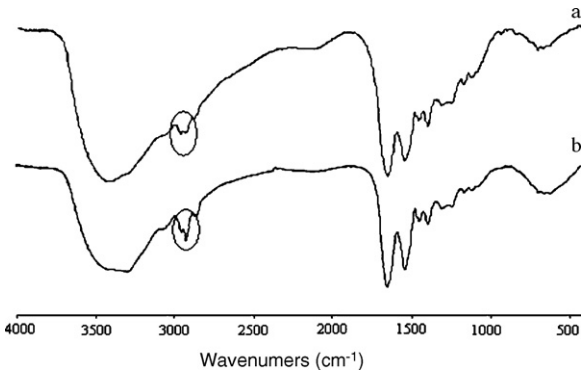

Fig. 1. IR spectra of BSA (a) and OSA-8 (b).

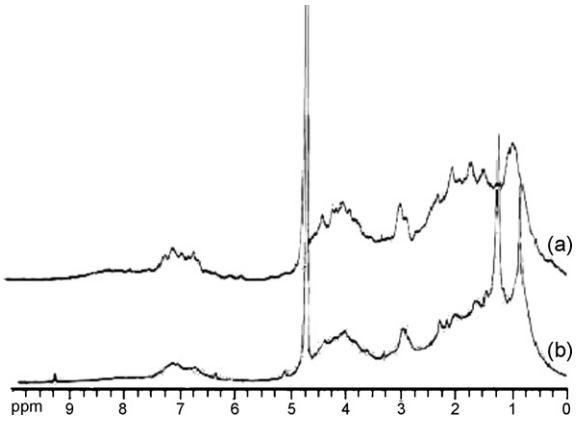

Fig. 2. ^{1}H NMR spectra of BSA (a) and OSA-8 (b).

different methods in this paper. Elemental analysis is a typical method to calculate the degree of substitution (Senso et al., 2000), however, not all of the nitrogen atoms can react with the aldehyde group in this situation, we modified the equation via multiplying by a correction factor. Fluorescamine assay is based on the direct proportion between the primary amine concentration and the fluorescence which result from the specific reaction between fluorescamine and primary amine (Stocks et al., 1986). DS of octyl group of OSAs obtained from elemental analysis and fluorescamine assay methods was in the range of 52.4–69.7% and 48.9–65.8%, respectively (Table 1). It can be seen that DS values measured by elemental analysis are a little bit higher than those measured by fluorescamine assay. This may be explained by the compact structure of BSA, which leads to fluorescamine not approachable to those reactable amino groups. Moreover, albumin molecule is a compact heart-shaped structure, so octaldehyde is not approachable to all primary amino groups, especially those inside the molecule, which makes the DS of octyl group low. However, the drug-loading capacity of a carrier is affected by the balance of hydrophobic and hydrophilic group, a over high DS of octyl group may disrupt the hydrophile–lipophile balance, consequently, leads to the precipitation of carrier and the decrease of its drug-loading capacity.

Table 1
The average size, polydispersity, zeta potential, DS of octyl group and CMC of a series of OSA. The size and zeta potential values represent the mean ± S.D. from five independent experiments.

Sample	d[a] (nm) (μ_2/Γ^2[b])	Zeta potential	DS (%)		CMC (mg/L)
			EA[c]	FA[d]	
OSA-2[e]	183.8 ± 7.8(0.25)	−27.4 ± 2.8	52.4	48.9	30.1
OSA-4[e]	165.0 ± 4.9(0.20)	−30.2 ± 1.6	58.2	54.6	20.2
OSA-6[e]	162.8 ± 5.8(0.22)	−28.5 ± 2.4	63.9	60.8	17.8
OSA-8[e]	158.5 ± 4.6(0.21)	−30.8 ± 1.9	69.7	65.8	14.7

[a] Mean diameters of micelles.
[b] Polydispersity index of micelles size.
[c] DS of octyl group measured by elemental analysis.
[d] DS of octyl group measured by fluorescamine assay.
[e] The number is representative of the molar ratio of aldehyde group to reactable amino group of BSA.

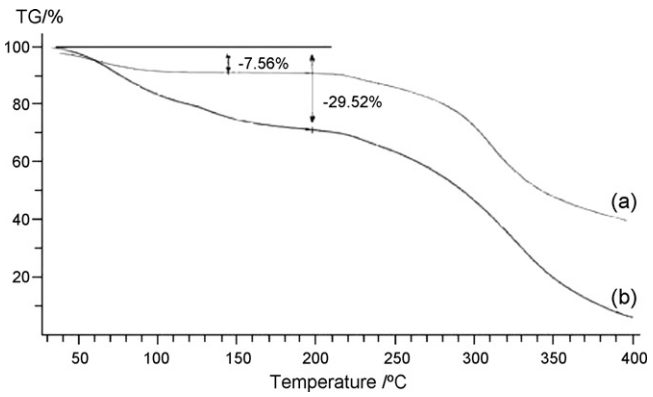

Fig. 3. TG thermograms of BSA (a) and OSA-8 (b).

Thermographs of BSA and OSA-8 are shown in Fig. 3. The tendency of BSA and OSA is similar except the initial and overall weight loss. OSA lost 29.5% of its weight while only 7.6% for BSA at first, due to the attached octyl group and the resultant unstable structure, which could indicate that OSA is less thermally stable than BSA.

The mean diameters (Table 1) of the polymeric micelles measured by a DLS analyzer were in the range of 158.5–183.8 nm with the polydispersity index smaller than 0.25, implying a narrow size distribution. The size decreased with the increase of octaldehyde feed amount owing to the strengthened hydrophobic interaction. The micelles were negatively charged due to the low p*I* of BSA. All of the zeta potentials were approximately −30 mV, which indicates the aqueous stability for the micelles. In terms of the morphology studies, spherical particles with core–shell structure and "spikes" which are contributive to the side chains of OSA are visualized by TEM (Fig. 4(a) and (b)). However, their sizes (about 120 nm) were smaller than those measured by DLS, which may be ascribed to the different state of the micelles. The size determined by TEM is the actual diameter (dry state), while that by DLS method is the hydrodynamic diameter (hydrated state), which is larger than the actual diameter for the solvent effect of the sample in the hydrated state.

CMC value is a parameter indicative of the micelle's stability upon the dilution of the blood and is obtained from the inflection point of the curve plotted by the intensity ratio I_{338}/I_{333} versus the logarithm of the concentration of polymeric micelles by fluorescence technique using pyrene as a probe. CMC values of OSAs (Table 1) decrease from 30.1 to 14.7 mg/L as the DS of octyl group increased, that is because higher hydrophobicity induced by more octaldehyde makes the formation of micelles more readily, which results in the lower CMC. The low CMC value enables the use of these novel micelles as drug carriers in much diluted conditions. Compared with some other studied polymeric micelles (15.0 mg/L for pHPMAmDL-*b*-PEG (Soga et al., 2004) and 85.5 mg/L for PEG_{5000}-*b*-$P(2\text{-VBOPNA})_{2400}$ (Kang Moo et al., 2008)), the CMC values of OSAs are in the same order of magnitude and are much lower than that of low-molecular weight surfactant (e.g. 1.0–24.0 × 10^3 mg/L for poloxamer (Prasad et al., 1982)).

3.2. PTX-loaded micelles

PTX was physically incorporated within the hydrophobic cores of the polymeric micelles using dialysis method; an opalescent

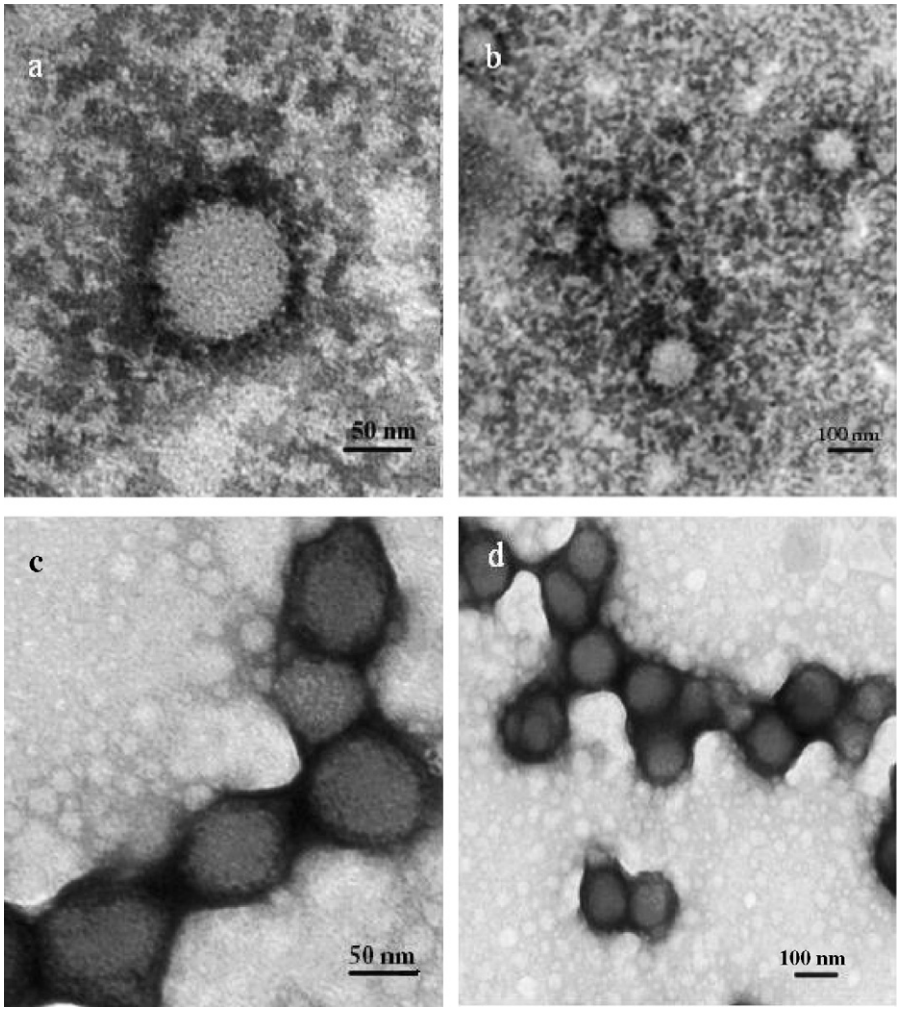

Fig. 4. Transmission electron microscopic (TEM) images of OSA-8 micelles without ((a) and (b)) and with ((c) and (d)) PTX.

and homogenous solution was obtained. Drug-loading capacities of the OSAs and unmodified BSA are listed in Table 2. Because of the low solubility of PTX in water, insignificantly compared to the amount dissolved in polymeric micelles, the amount of free PTX was not taken into account when calculating the drug-loading and entrapment efficiency. The drug-loading capacity enhanced with the increasing of the DS of octyl group in OSA, e.g. the drug-loading of OSA-8 was 33.1 wt%, while that of unmodified BSA was only 24.6 wt%. This result could be explained by the fact that the higher the DS of octyl group in OSA, the stronger binding affinity between PTX and the hydrophobic segment due to the hydrophobic character of PTX. Consequently, in this micellar system, the maximum drug-loading was 33.1 wt% with an entrapment efficiency of 90.5%, obtained from OSA-8, which was characterized by the highest hydrophobicity. Moreover, the drug-loading capacity was higher than some other reported micelles, such as pHPMAmDL-*b*-PEG (22.0 wt%) (Soga et al., 2005), PLA-PEG (25.0 wt%) (Zhang et al., 1996) and albumin-bound nanoparticle paclitaxel (16.6 wt%) (Zenoni and Maschio, 2007). Such a high drug-loading capacity was considered as a result of the synergistic effect of the

Table 2
The average size, polydispersity, zeta potential, drug-loading, entrapment efficiency and stability of a series of PTX-loaded micelles. The size, zeta potential, DL and EE values represent the mean ± S.D. from five independent experiments.

Sample	d[a] (nm) (μ_2/Γ^2[b])	Zeta potential	DL (wt%)[c]	EE (%)[c]	Stability[d] (day)		
					4 °C	25 °C	37 °C
OSA-0	171.8 ± 8.6(0.17)	−32.5 ± 4.1	24.6 ± 1.8	58.7 ± 5.6	18	3	1
OSA-2[e]	152.8 ± 4.9(0.13)	−33.0 ± 2.7	31.0 ± 0.9	81.8 ± 3.4	20	4	1.5
OSA-4[e]	147.4 ± 6.8(0.12)	−41.3 ± 1.9	31.7 ± 0.6	84.8 ± 2.4	26	5	2
OSA-6[e]	143.0 ± 3.4(0.11)	−43.6 ± 2.5	32.2 ± 0.3	85.8 ± 1.1	35	7	3
OSA-8[e]	123.2 ± 5.7(0.14)	−39.9 ± 3.6	33.1 ± 0.7	90.5 ± 2.9	>35	9	5

[a] Mean diameters of micelles.
[b] Polydispersity index of micelles size.
[c] DL and EE are short for drug-loading and entrapment efficiency, respectively.
[d] Stability measured as time when PTX content less than 90%.
[e] The number is representative of the molar ratio of aldehyde group to reactable amino group of BSA.

unique micellar encapsulation and the binding interaction between drug and OSA due to the high protein binding rate (89–98%) of PTX.

It is noted that the size of a colloidal drug carrier is a determinant feature of its fate in blood circulation and its biodistribution. A small size may avoid the non-selective recognition by the reticuloendothelial system (RES) and result in a long blood circulation. Meanwhile, particle size distribution is crucial in particle distribution, because size-sieving may occur during the distribution process in the body. Thus, a narrow size distribution is desired for carrier particle in order to accomplish selective accumulation at target site. The sizes of PTX-loaded OSA micelles (Table 2) were in the range of 123.2–171.8 nm with narrow size distributions, which is reasonably assume a increasing accumulation in tumor tissue because of the EPR effect. Moreover, the size decreased with the increasing of DS of octyl group, which indicates that more compact hydrophobic cores have formed because of the increasing hydrophobic interaction. The size of PTX-loaded micelles is smaller than its corresponding blank micelles, indicating the addition of hydrophobic drug may induce the micelles more compact by the hydrophobic interaction between PTX and the hydrophobic segments of the micelles. The morphology (Fig. 4(c) and (d)) is identical to that of blank micelles. However, absolute value of zeta potentials was increased after drug-loading, which may be attributed to the changed microstructure of OSA micelles upon drug-loading and the decreased positive charge of OSA binding entrances due to PTX binding. The increased absolute value of zeta potential indicated an enhanced aqueous stability for the PTX-loaded micelles.

The stability of PTX-loaded preparations in terms of PTX content is shown in Table 2. It can be seen that PTX-loaded OSA-8 and BSA preparations are stable until more than 35 days versus 18 days, 9 days versus 3 days and 5 days versus 1 day at 4, 25 and 37 °C, respectively. The result indicated that PTX-loaded OSA micelles were more stable than PTX-loaded unmodified BSA preparation. This may be explained by the fact of the stronger hydrophobic interaction between PTX and the hydrophobic segment of OSA. Meanwhile, it is seen that no significant changes are observed in the size of blank micelles (date not shown) during the follow-up period, which indicates that the relative instability of PTX-loaded micelles was not induced by the aggregation of micelles but by the release of PTX from micelles.

WAXD and DSC diagrams of OSA-8, PTX, physical mixture of PTX and OSA-8 and PTX-loaded OSA-8 micelles are shown in Figs. 5 and 6, respectively. From the WAXD diagram of PTX (Fig. 5(b)), we can see three intense peaks at 2θ of 5.28°, 8.84°and 12.26° and numerous small peaks between 15° and 25°. The endothermic peak at 224.2 °C and the exothermic peak at 244.5 °C in the DSC thermogram of PTX (Fig. 6(b)) are attributed to melting and decomposition of PTX, respectively. These characteristic WAXD and DSC peaks of PTX do not exist in the diagrams of PTX-loaded OSA-8 micelles, but in those of physical mixture of PTX and OSA-8, which suggests that PTX exist in the micelles with the state of amorphism or solid dispersion.

3.3. Hemolysis test

Since the amphiphilic compounds could solubilize lipids or be inserted into phospholipid membranes to destabilize them, consequently, leads to hemolysis of RBC, hemolysis test is necessary for new amphiphilic compounds. The hemolysis of OSA was compared with the vehicle of the commercial PTX formulation CrmEL and common used low-molecular weight surfactant Tween-80 (Fig. 7(a)). It can be observed that the hemolysis of OSA was negligible, even at concentration up to 4 mg/mL and similar to that of CrmEL while the hemolysis of Tween-80 was sharply increased at the concentration above 0.6 mg/mL and was 57.4% at the concentration of 4 mg/mL. However, CrmEL is hypersensitive with a MTD of 75 mg/day (Miwa et al., 1998).

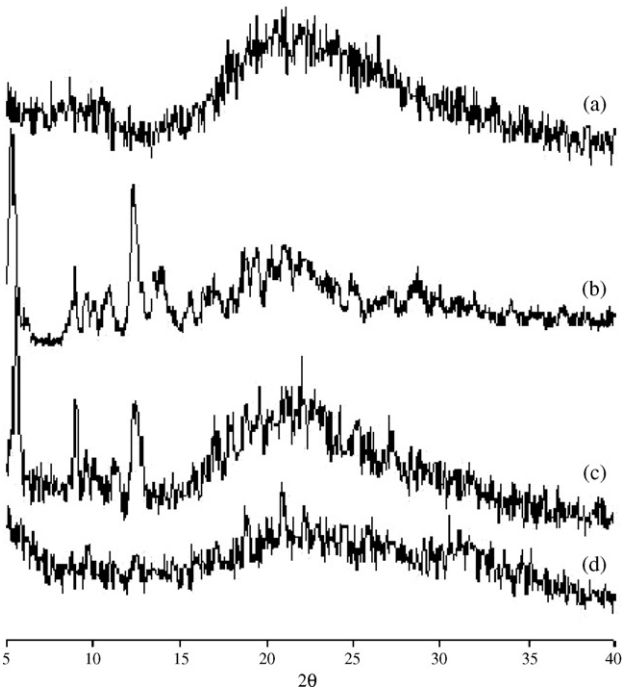

Fig. 5. Power X-ray diffraction patterns of OSA-8 (a), PTX (b), physical mixture of PTX and OSA-8 (c) and PTX-loaded OSA-8 micelles (d).

Meanwhile, the hemolysis of PTX-loaded OSA was compared with the commercial PTX formulation Taxol® (Fig. 7(b)). PTX-loaded OSA demonstrated an insignificant hemolytic activity, with only 2.4% at the concentration of 0.2 mg/mL, while 11.8% for Taxol®, suggesting that OSA micelles would be nontoxic towards erythrocytes after intravenous injection.

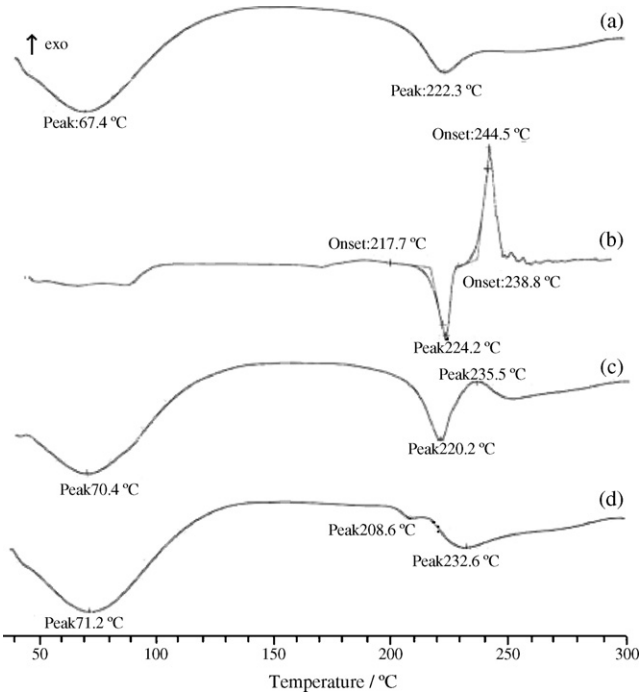

Fig. 6. DSC thermograms of OSA-8 (a), PTX (b), physical mixture of PTX and OSA-8 (c) and PTX-loaded OSA-8 micelles (d).

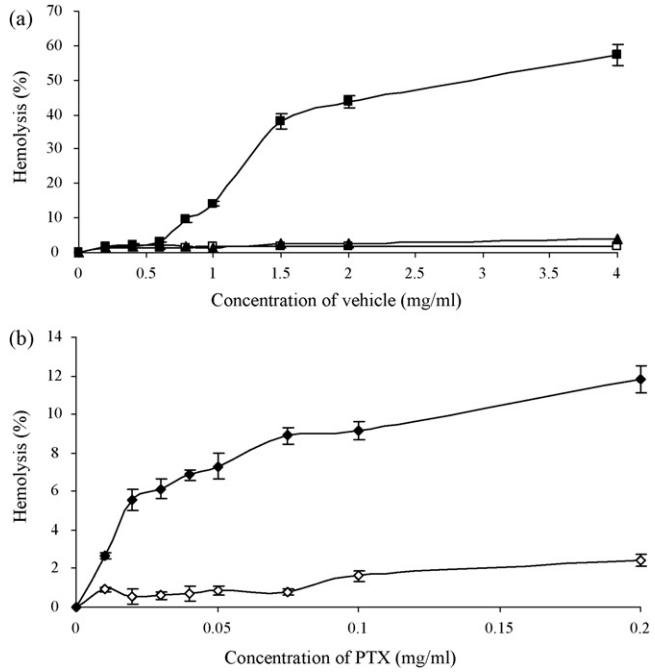

Fig. 7. Hemolysis as a function of vehicle concentration of OSA (□), Tween-80 (■) and CrmEL (▲) (a) and PTX concentration of PTX-loaded OSA micelles (◊) and Taxol® (♦) (b). Each datum represents the mean value ± S.E. from three independent experiments.

3.4. In vitro cytotoxicity studies

The cytotoxicity of PTX-loaded OSA micelles and Taxol® was evaluated with Hepg2 cells at the PTX concentration between 0.0001 and 100 μg/mL. Meanwhile, that of the blank micelles and Taxol® vehicle with the corresponding concentration were also studied. As shown in Fig. 8, the cell viabilities of blank OSA micelles were approximately 100% even at the highest concentration tested, while those of Taxol® vehicle were 53.1% and 70.8% at the vehicle concentration of 200 and 2 μg/mL, respectively. From the hemolysis and cytotoxicity studies of OSA, it could be tentatively concluded that OSA is a safer injectable pharmaceutic adjuvant and PTX-loaded OSA preparation could possess a high MTD, which enables a high dose in clinical use according to the standard medical oncology practice, consequently results in a higher response rate and a lower incidences of adverse effect than the commercial available formulation (Taxol®).

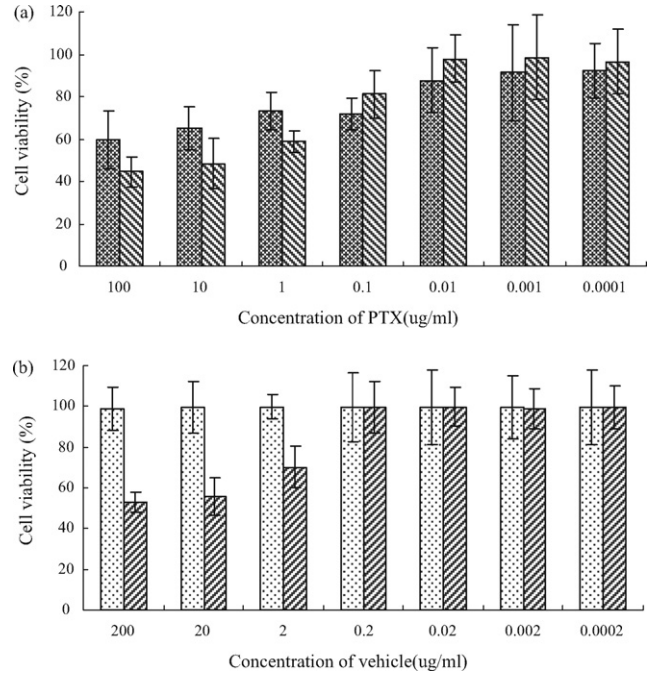

Fig. 8. Viability of Hepg2 cells as a function of PTX concentration of PTX-loaded OSA micelles ( ) and Taxol® ( ) (a), and corresponding concentration of blank OSA micelles ( ) and Taxol® vehicle ( ) (b). Each datum represents the mean value ± S.E. from six independent experiments.

PTX-loaded OSA exhibited a greater antitumor activity than Taxol® at a low concentration of PTX which indicates that the OSA micelles have an insignificant effect on the antitumor activity of PTX, while at a high concentration the antitumor activity of PTX-loaded OSA was less than Taxol®; nevertheless, the cytotoxicity of Taxol® may be attributive to CrmEL rather than PTX, because the cytotoxic profile of Taxol® was same as that of the blank vehicle. However, for its low volume of distribution, CrmEL remains within the vasculature compartment largely rather than the tumor tissues (Sparreboom et al., 1998), consequently, the in vivo antitumor efficacy was modest while the toxic effect was severe even with a high AUC (Kim et al., 2001). Moreover, PTX-loaded OSA micelles have a higher potential antitumor efficacy owing to the combined effect of pathophysiology of tumor tissue, i.e. tumor EPR effect, which is characterized by hypervascularization, a defective vascular architecture and an impaired lymphatic drainage (Fang et al., 2003) and the receptor-activated transcytosis by gp60 receptor (albondin) (Simionescu et al., 2002) and SPARC (secreted protein acid and rich in cysteine) (Porter et al., 1995). In terms of its safe character as well as the higher potential antitumor efficacy, it can be suggested that OSA was a promising adjuvant for PTX formulation.

4. Conclusions

A novel polymer which can form a core–shell structure due to its amphiphilicity in aqueous media has been prepared by using serum albumin and octaldehyde with a CMC of 14.7 mg/L. PTX was successfully loaded into OSA micelles with a higher drug-loading (33.1 wt%) and entrapment efficiency (90.5%) due to the synergistic effect of the micellar encapsulation and the binding interaction between drug and OSA. Compared with PTX-loaded unmodified BSA preparation, PTX-loaded OSA micelles possessed a smaller size, a narrower size distribution, a greater drug-loading capacity and a more stable character. Hemolysis and cytotoxicity studies indicated that OSA was safer than Tween-80 and CrmEL as an injectable pharmaceutic adjuvant for PTX. In terms of the greater drug-loading capacity and safer character, it is worthy of being studied further as a carrier for hydrophobic drugs. The pharmacokinetics, biodistribution and efficacy of PTX-loaded OSA micelles will be further studied.

References

Aliabadi, H.M., Lavasanifar, A., 2006. Polymeric micelles for drug delivery. Expert Opin. Drug Deliv. 3, 139–162.
Bilensoy, E., Gürkaynak, O., Dogan, A.L., Hincal, A.A., 2008. Safety and efficacy of amphiphilic β-cyclodextrin nanoparticles for paclitaxel delivery. Int. J. Pharm. 347, 163–170.
Bouquet, W., Boterberg, T., Ceelen, W., Pattyn, P., Peeters, M., Bracke, M., Remon, J.P., Vervaet, C., 2009. In vitro cytotoxicity of paclitaxel/beta-cyclodextrin complexes for HIPEC. Int. J. Pharm. 367, 148–154.
Carter, D.C., Ho, J.X., 1994. Structure of serum albumin. Adv. Protein Chem. 45, 153–203.
Chemmanur, A.T., Wu, G.Y., 2006. Drug evaluation: albuferon-alpha—an antiviral interferon-alpha/albumin fusion protein. Curr. Opin. Investig. Drugs 7, 750–758.
Fang, J., Sawa, T., Maeda, H., 2003. Factors and mechanism of "EPR" effect and the enhanced antitumor effects of macromolecular drugs including SMANCS. Adv. Exp. Med. Biol. 519, 29–49.
Figge, J., Rossing, T.H., Fencl, V., 1991. The role of serum proteins in acid–base equilibria. Lab. Clin. Med. 117, 453–467.

Gelderblom, H., Verweij, J., Nooter, K., Sparreboom, A., 2001. Cremophor EL: the drawbacks and advantages of vehicle selection for drug formulation. Eur. J. Cancer 37, 1590–1598.

Ghuman, J., Zunszain, P.A., Petitpas, I., Bhattacharya, A.A., Otagiri, M., Curry, S., 2005. Structural basis of the drug-binding specificity of human serum albumin. J. Mol. Biol. 353, 38–52.

He, L., Wang, G.-l., Zhang, Q., 2003. An alternative paclitaxel microemulsion formulation: hypersensitivity evaluation and pharmacokinetic profile. Int. J. Pharm. 250, 45–50.

He, X.M., Carter, D.C., 1992. Atomic structure and chemistry of human serum albumin. Nature 358, 209–215.

Ibrahim, N.K., Desai, N., Legha, S., Soon-Shiong, P., Theriault, R.L., Rivera, E., Esmaeli, B., Ring, S.E., Bedikian, A., Hortobagyi, G.N., Ellerhorst, J.A., 2002. Phase I and pharmacokinetic study of ABI-007, a Cremophor-free, protein-stabilized. Nanoparticle formulation of paclitaxel. Clin. Cancer Res. 8, 1038–1044.

Kang Moo, H., Hyun Su, M., Sang Cheon, L., Hong Jae, L., Sungwon, K., Kinam, P., 2008. A new hydrotropic block copolymer micelle system for aqueous solubilization of paclitaxel. J. Control. Release 126, 122–129.

Kataoka, K., Harada, A., Nagasaki, Y., 2001. Block copolymer micelles for drug delivery: design, characterization and biological significance. Adv. Drug Deliv. Rev. 47, 113–131.

Kim, S.C., Kim, D.W., Shim, Y.H., Bang, J.S., Oh, H.S., Kim, S.W., Seo, M.H., 2001. In vivo evaluation of polymeric micellar paclitaxel formulation: toxicity and efficacy. J. Control. Release 72, 191–202.

Kim, T.-Y., Kim, D.-W., Chung, J.-Y., Shin, S.G., Kim, S.-C., Heo, D.S., Kim, N.K., Bang, Y.-J., 2004. Phase I and pharmacokinetic study of Genexol-PM, a cremophor-free, polymeric micelle-formulated paclitaxel, in patients with advanced malignancies. Clin. Cancer Res. 10, 3708–3716.

Kratz, F., 2007. DOXO-EMCH (INNO-206): the first albumin-binding prodrug of doxorubicin to enter clinical trials. Expert Opin. Investig. Drugs 16, 855–866.

Kratz, F., 2008. Albumin as a drug carrier: design of prodrugs, drug conjugates and nanoparticles. J. Control. Release 132, 171–183.

Miwa, A., Ishibe, A., Nakano, M., Yamahira, T., Itai, S., Jinno, S., Kawahara, H., 1998. Development of novel chitosan derivatives as micellar carriers of taxol. Pharm. Res. 15, 1844–1850.

Peters, T., 1985. Serum albumin. Adv. Protein Chem. 37, 161–245.

Porter, P.L., Sage, E.H., Lane, T.F., Funk, S.E., Gown, A.M., 1995. Distribution of SPARC in normal and neoplastic human tissue. J. Histochem. Cytochem. 43, 791–800.

Prasad, K.N., Luong, T.T., Florence, A.T., Paris, J., Vautin, C., Seiller, M., Puisieux, F., 1982. Surface activity and association of ABA polyoxyethylene–polyoxypropylene block copolymers in aqueous solution. J. Colloid. Interface Sci. 90, 303–309.

Senso, A., Franco, P., Oliveros, L., Minguillon, C., 2000. Characterization of doubly substituted polysaccharide derivatives. Carbohydr. Res. 329, 367–376.

Simionescu, M., Gafencu, A., Antohe, F., 2002. Transcytosis of plasma macromolecules in endothelial cells: a cell biological survey. Microsc. Res. Technol. 57, 269–288.

Skwarczynski, M., Noguchi, M., Hirota, S., Sohma, Y., Kimura, T., Hayashi, Y., Kiso, Y., 2006. Development of first photoresponsive prodrug of paclitaxel. Bioorg. Med. Chem. Lett. 16, 4492–4496.

Soga, O., van Nostrum, C.F., Fens, M., Rijcken, C.J.F., Schiffelers, R.M., Storm, G., Hennink, W.E., 2005. Thermosensitive and biodegradable polymeric micelles for paclitaxel delivery. J. Control. Release 103, 341–353.

Soga, O., van Nostrum, C.F., Ramzi, A., Visser, T., Soulimani, F., Frederik, P.M., Bomans, P.H., Hennink, W.E., 2004. Physicochemical characterization of degradable thermosensitive polymeric micelles. Langmuir 20, 9388–9395.

Sparreboom, A., Scripture, C.D., Trieu, V., Williams, P.J., De, T., Yang, A., Beals, B., Figg, W.D., Hawkins, M., Desai, N., 2005. Comparative preclinical and clinical pharmacokinetics of a cremophor-free. Nanoparticle albumin-bound paclitaxel (ABI-007) and paclitaxel formulated in Cremophor (Taxol). Clin. Cancer Res. 11, 4136–4143.

Sparreboom, A., Verweij, J., van der Burg, M.E., Loos, W.J., Brouwer, E., Vigano, L., Locatelli, A., de Vos, A.I., Nooter, K., Stoter, G., Gianni, L., 1998. Disposition of Cremophor EL in humans limits the potential for modulation of the multidrug resistance phenotype in vivo. Clin. Cancer Res. 4, 1937–1942.

Spencer, C.M., Faulds, D., 1994. Paclitaxel. A review of its pharmacodynamic and pharmacokinetic properties and therapeutic potential in the treatment of cancer. Drugs 48, 794–847.

Stocks, S.J., Jones, A.J.M., Ramey, C.W., Brooks, D.E., 1986. A fluorometric assay of the degree of modification of protein primary amines with polyethylene glycol. Anal. Biochem. 154, 232–234.

Sugio, S., Kashima, A., Mochizuki, S., Noda, M., Kobayashi, K., 1999. Crystal structure of human serum albumin at 2.5 A resolution. Protein Eng. 12, 439–446.

Veronese, F.M., 2001. Peptide and protein PEGylation: a review of problems and solutions. Biomaterials 22, 405–417.

Wu, J., Liu, Q., Lee, R.J., 2006. A folate receptor-targeted liposomal formulation for paclitaxel. Int. J. Pharm. 316, 148–153.

Zenoni, M., Maschio, S., 2007. Paclitaxel-based antitumor formulation. USA Patent US 2 007 020 337 A1, 25 January (2007).

Zhang, X., Jackson, J.K., Burt, H.M., 1996. Development of amphiphilic diblock copolymers as micellar carriers of taxol. Int. J. Pharm. 132, 195–206.